MICROSCOPY RESEARCH AND TECHNIQUE 75:74–80 (2012)

Ultrastructure of Spermatozoa in Two Solitary Bee Species With an Emphasis on Synapomorphic Traits Shared in the Family Apidae

VINÍCIUS ALBANO ARAÚJO,[1]* JOSÉ EDUARDO SERRÃO,[2] JANE MOREIRA,[3]
SÔNIA NAIR BÁO,[4] AND JOSÉ LINO-NETO[2]
[1]*Instituto de Ciências Biológicas e da Saúde, Universidade Federal de Viçosa/Campus Rio Paranaíba, Minas Gerais, CEP: 38810-000, Brazil*
[2]*Departamento de Biologia Geral, Universidade Federal de Viçosa, Minas Gerais, CEP: 36570-000, Brazil*
[3]*Departamento de Biologia Animal, Universidade Federal de Viçosa, Minas Gerais, CEP: 36570-000, Brazil*
[4]*Departamento de Biologia Celular, Universidade de Brasília, Distrito Federal, CEP: 70919-970, Brazil*

KEY WORDS centriolar adjunct; synapomorphy; phylogeny; apoidea

ABSTRACT Morphology of spermatozoa in bees has provided promising results for phylogenetic analyses. In this work, the structure and ultrastructure of spermatozoa from *Thygater (Thygater) analis* and *Melitoma segmentaria* were characterized and the synapomorphies shared in the family Apidae are discussed. In these species, spermatozoa bundles which are undone in the seminal vesicle possess, on average, 50 cells. Spermatozoa consist of a head and a flagellar region. The head includes an acrosome containing the perforatorium, covered by the acrosomal vesicle and a nucleus. The flagellum is formed by two mitochondrial derivatives, which are asymmetric in diameter and length, with one centriolar adjunct, one axoneme (9 + 9 + 2), and two accessory bodies. In cross section the centriolar adjunct is asymmetric and the accessory bodies are triangular in shape. In the distal region of the flagellum, the derivative terminates before the axoneme and the small derivative terminates first. The axoneme is gradually disorganized and the accessories microtubules are the last to terminate. In these two species, spermatozoa share diverse synapomorphies with those of other bee species previously described in the literature, which allows for the establishment of a morphological pattern for spermatozoa of the family Apidae. *Microsc. Res. Tech. 75:74–80, 2012.* © 2011 Wiley Periodicals, Inc.

INTRODUCTION

The morphology of insect spermatozoa is important for distinguishing traits for phylogenic analyses at different taxonomic levels (Baccetti, 1970; Dallai, 1974; Dallai and Afzelius, 1993; Jamieson, 1987; Jamieson et al., 1999; Phillips, 1970). The first comparative morphology study of spermatozoa in Hymenoptera was performed by Quicke et al. (1992), with species from 14 families representing symphyta, both Aculeata and Parasitica. Jamieson et al. (1999) proposed a phylogeny for endopterygota utilizing morphological and molecular traits, in addition to apomorphic traits of spermatozoa for each order. These authors suggest that "perforatorium inserted in a small cavity on the anterior extremity of the nucleus" is the only apomorphic characteristic of spermatozoa in Hymenoptera.

In bees, the ultrastructure of spermatozoa has been described in species of Apinae (Araújo et al., 2005a; Báo et al., 2004; Cruz-Hofling et al., 1970; Hoage and Kessel, 1968; Lensky et al., 1979; Lino-Neto et al., 2000; Peng et al., 1992, 1993; Quicke et al., 1992; Rothschild, 1955; Woyke, 1984; Zama et al., 2001, 2004, 2005a,b), Halictinae (Fiorillo et al., 2005), Megachilinae and Andreninae (Gracielle et al., 2009; Quicke et al., 1992). In these bees, spermatozoa present a common short head region, formed by the acrosome and nucleus, and a flagellum region composed of two asymmetric mitochondrial derivatives, one centriolar adjunct, one axoneme with a microtubule arrangement of 9 + 9 + 2 and two accessory bodies. In bees, as in Aculeata in general, spermatozoa are transferred to the seminal vesicles in bundles (spermatodesm), which are disrupted during sexual maturation (Araújo et al., 2005b; Moreira et al., 2004, 2008).

In this study, the ultrastructure of spermatozoa in two Apinae species were characterized and compared with those of other species previously published to investigate synapomorphic characteristics for bees. This provides an ultrastructural pattern for spermatozoa in the Apidae family.

---

*Correspondence to: Vinícius Albano Araújo, Instituto de Ciências Biológicas e da Saúde Universidade Federal de Viçosa/Campus Rio Paranaíba, Rodovia BR 354 - Km 310, Rio Paranaíba, Minas Gerais, CEP: 38810-000, Brazil.
E-mail: viniciusalbano@ufv.br

Received 2 February 2011; accepted in revised form 6 April 2011

Contract grant sponsor: CNPq; Contract grant number: Proc. 142455/2005-9; Contract grant sponsor: Conselho Nacional de Desenvolvimento Científico e Tecnológico; Contract grant sponsor: Coordenação de Aperfeiçoamento de Pessoal de Nível Superior; Contract grant sponsor: CAPES (Procad)

DOI 10.1002/jemt.21027

MATERIALS AND METHODS

Eight adult males of *Thygater (Thygater) analis* (Lepeletier 1841) and of *Melitoma segmentaria* (Fabricius 1804) were collected with entomological nets while visiting *Ipomoea* sp. (Convolvulaceae) flowers on the campus of the Federal University of Viçosa, Minas Gerais, Brazil.

Light Microscopy

For each male, the suspension of spermatozoa extracted from one of the seminal vesicles was spread on clean glass microscope slides and fixed for 20 min in a solution of 4% (wt/vol) paraformaldehyde in 0.1 M sodium phosphate buffer (PBS), pH 7.2. After drying at room temperature, the preparations were observed with a photomicroscope (Olympus, BX-60), equipped with phase contrast and 50 spermatozoa were photographed to be measured. To access nucleus measurements, some of these preparations were stained for 15 min with 0.2 μg/mL 4,6-diamino-2-phenylindole (DAPI) in PBS, washed, and mounted in 50% sucrose. They were examined with an epifluorescence microscope (Olympus, BX-60), equipped with a BP360–370 nm excitation filter and 50 nuclei were photographed. All the measurements were obtained with the software Image Pro-Plus, version 4.5 (Media Cybernetics, MD) and the lengths were averaged from the total number of spermatozoa analyzed.

Transmission Electron Microscopy (TEM)

From each male, one of the seminal vesicles was fixed for 24 h, at 4°C, in a solution containing 2.5% glutaraldehyde, 0.2% picric acid, 3% sucrose, and 5 mM $CaCl_2$ in 0.1 M sodium cacodylate buffer at pH 7.2. After rinsing buffer, they were postfixed with 1% osmium tetroxide in the same buffer for 2 h. Dehydration was carried out in acetone, followed by embedding in Epon 812 resin. Ultrathin sections were stained with the 2% uranyl acetate and 0.2% lead citrate in 1 M sodium hydroxide and observed with the Zeiss EM 109 transmission electron microscope.

RESULTS

Spermatozoa from *T. analis* and *M. segmentaria* are long, slender and measure, on the average, 500 μm and 300 μm in length, respectively (Figs. 1A and 1C). In *T. analis* the nucleus is on the average, 45 μm in length (Fig. 1B) with a nucleus/flagellum length ratio of 0.09, whereas in *M. segmentaria* the nucleus is on the average 30 μm in length (Fig. 1D) and the nucleus/flagellum ratio is equal to 0.1.

Spermatozoa of both *T. analis* and *M. segmentaria* exit the testes in bundles and become frequently undone in the seminal vesicle lumen (Fig. 1E). However, the bundles or their fragments are sometimes observed in the seminal vesicle (Figs. 1F–1G). Spermatozoa arranged in bundles are maintained by a fibrous cap of extracellular material in which the anterior portion of the sperm heads (acrosome and part of the nucleus) are embedded (Fig. 1F). These bundles possess, on the average, 50 spermatozoa (Fig. 1G).

The head region of the spermatozoa consists of an acrosomal complex and the nucleus (Figs. 1H–1K). The acrosome measures ~1.8 μm in both species and is composed of a cone shaped acrosomal vesicle which covers the perforatorium, and spans its entire length (Figs. 1I–1J). The base of the perforatorium is inserted into a cavity at the anterior nucleus tip (Fig. 1K). This cavity measures ~0.2 μm in *T. analis* (Fig. 1K) and 0.18 μm in *M. segmentaria*. In cross section, we observed that an acrosomal vesicle is formed by the lamellar structure (Figs. 1L–1Q). Cross sections of the acrosomal vesicle are circular in the anterior region and become oval in shape toward the nucleus (Figs. 1L–1Q). Along the acrosome, an electron-lucid layer separates the perforatorium from the acrosomal vesicle (Figs. 1J and 1O–1P).

The nucleus is linear and electron-dense, with many electron-lucid lacunae, principally in the peripheral regions spanning its length (Figs. 2A and 2B). In cross section, the nucleus presents an oval shape (Fig. 2B). The posterior extremity of the nucleus is asymmetric and positioned parallel to the anterior region of the axoneme and at the top of the large mitochondrial derivative (Figs. 2C–2E).

The centriolar adjunct begins at the nuclear base, extends parallel to the axoneme and large mitochondrial derivative (Figs. 2E–2F) and terminates just above the small mitochondrial derivative, which gives this adjunct an asymmetric pattern. In transverse section, the centriolar adjunct presents a triangular format and is compact and electron dense (Fig. 2F).

The flagellum consists of two accessory bodies, an axoneme and two mitochondrial derivatives. In cross section, the accessory bodies present triangular formats (Figs. 2H–2J) and are located between the axoneme and the mitochondrial derivatives, but are not found between the axoneme and the centriolar adjunct (Fig. 2F). In the anterior region, the axoneme began as an atypical centriole, without the central microtubules, since they begin posterior to the centriolar region (Figs. 2C–2D). The axoneme follows the typical 9 + 9 + 2 microtubule arrangement, where the nine single accessory microtubules are the most external and are followed by the nine doublets and a central pair (Figs. 2H and 3A–3B).

Mitochondrial derivatives are asymmetric in both size and diameter (Figs. 2H and 3A). Anteriorly, the large mitochondrial derivative begins adjacent to the nuclear extremity (Fig. 2C), while the small mitochondrial derivative begins immediately below the centriolar adjunct. Mitochondrial derivatives are divided into four regions: (1) a clear, circular, and centrally localized region; (2) an electron dense region adjacent to the axoneme; (3) a cristae region, which is confined to distal border in relation to the axoneme and (4) a paracrystalline region which is found only on the large mitochondrial derivative (Figs. 2H and 3C). In longitudinal sections, cristae are perpendicular along the axis of the derivatives and with regular interval spaces which measure 25 nm in *T. analis* (Fig. 2G) and 29 nm in *M. segmentaria*. In the final region of the flagellum, the derivatives terminate before the axoneme and the derivative with smallest diameter is the first to terminate (Figs. 2I–2K). The axoneme is the longest component of the flagellum, and in its posterior extremity, the microtubules are the last to terminate (Figs. 2K–2P). In the final region, the two central microtubules terminated

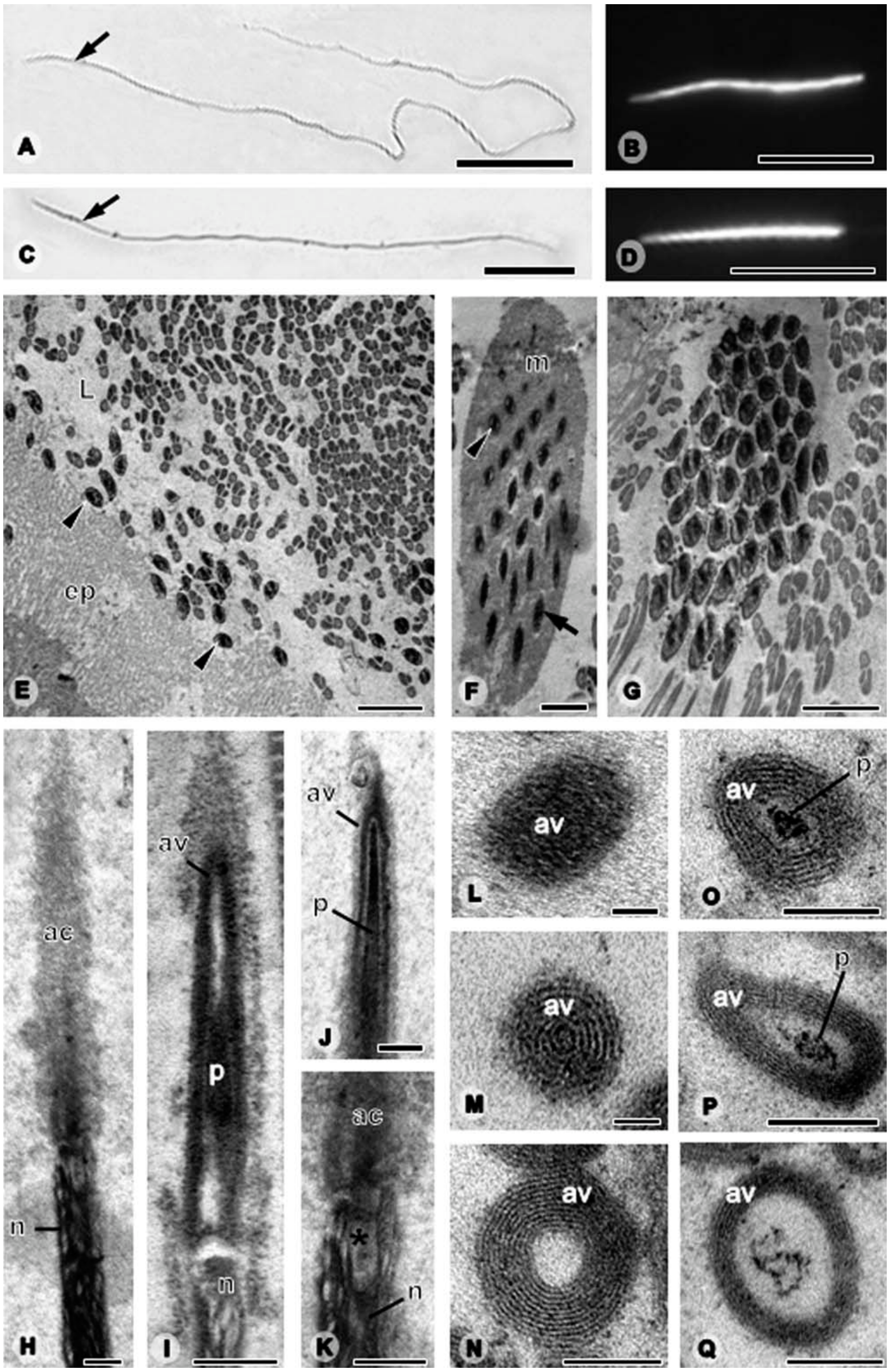

Fig. 1. A-B. Micrographs of *T. analis* spermatozoa. **A**: Phase contrast, the arrow indicates the limit between the head and the flagellum **B**: Head region, showing the nucleus stained with DAPI. **C**,**D**: Micrographs of *M. segmentaria* spermatozoa. C. Phase contrast, the arrow indicates the limit between the head and the flagellum. **D.** Head region, showing the nucleus stained with DAPI. **E–Q.** Transmission electron micrographs of the spermatozoa in the seminal vesicle of *T. analis*. **E.** Section of the seminal vesicle showing the epithelial region (ep) and the lumen (L) filled with spermatozoa; the arrowheads indicate sectioned spermatozoa in the nucleus region. **F**: Cross section of a spermatodesm, sectioned in the nucleus region (arrow) and acrosome (arrowhead) embedded in a less dense extracellular material matrix (m). **G**: Cross section of a spermatodesm at the height of the nuclei, with 50 spermatozoa. **H**: Longitudinal section of the anterior region of the head showing the acrosome (ac) and the nucleus (n). **I-J**: Longitudinal section of the acrosome indicating the acrosomal vesicle (av) and the perforatorium (p). **K**: Longitudinal section of the transition region between the acrosome (ac) and the nucleus (n), showing that the base of the perforatorium is established in a cavity at the tip of the nucleus (asterisk). L-Q**:** Cross sections from the anterior to posterior region for the acrosome, showing the acrosomal vesicle (av) and the perforatorium (p). Bar lengths: A and C = 50 μm; B and D = 20 μm; E and G = 2 μm; F = 1 μm; H-K = 0.2 μm; L-Q = 0.1 μm.

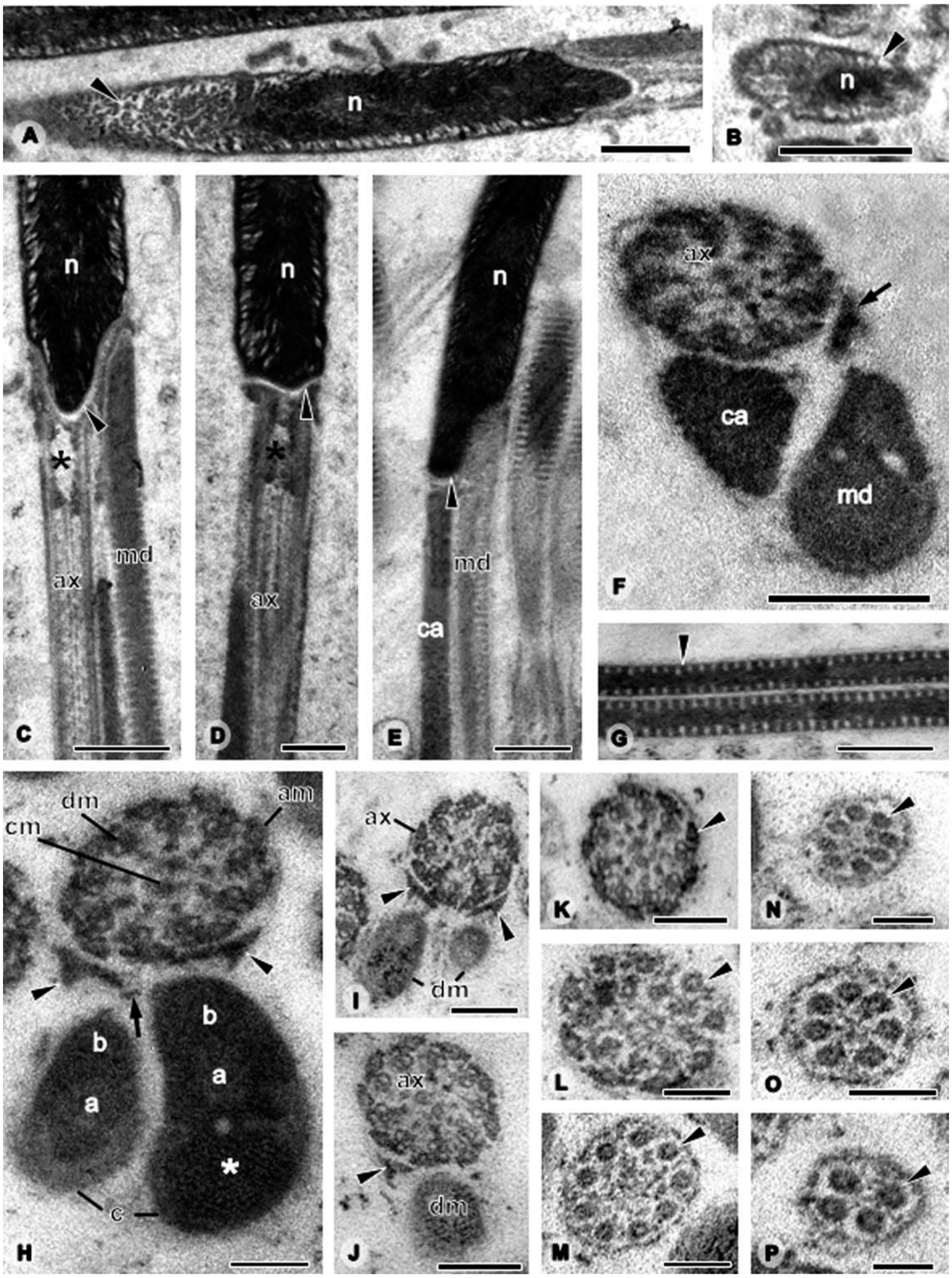

Fig. 2. Transmission electron micrographs of the spermatozoa in the seminal vesicle of *T. analis* (A-B and D-P) and *M. segmentaria* (C). **A**,**B**: Longitudinal and transversal sections, respectively, of the nucleus showing the electron lucid lacunae along the perimeter (arrowheads). **C–E**: Longitudinal sections of the nucleus-flagellum transition region. The arrowhead indicates the nucleus base (n). Note the posterior nuclear projection (arrowhead), the axoneme insertion (ax), the large mitochondrial derivative (md), the centriolar adjunct (ca) and the centriolar region of the flagellum (asterisk). **F**: Cross section of the flagellum showing a prominent centriolar adjunct (Ca) in the anterior portion of the flagellum, adjacent the axoneme (ax) and the large mitochondrial derivative (md) and an accessory body (arrow). **G**: Longitudinal section of the mitochondrial derivatives showing the cristae region (arrow). **H**: Cross section of the flagellum showing the axoneme with nine accessories microtubule (am), nine doublets (dm) and one central pair (cm). Arrowheads indicate the accessory bodies and arrows indicate a central material between flagellar structures. Both derivatives possess a less dense central area (a), an electron dense region adjacent to the axoneme (b) and a cristae region opposite the axoneme (c). The asterisk indicates a paracrystalline region present only in the large derivative. **I–P**: Cross sections of the posterior flagellar extremity. **I**: Showing the axoneme (ax), the mitochondrial derivatives (dm) and the accessory bodies (arrowheads). **J**: Showing the axoneme (ax) and a mitochondrial derivative (dm). Note that one derivative terminates before the other. An arrow indicates an accessory body. **K–P**: Disorganization of microtubules. The arrowheads indicate the accessories microtubules which are the last to terminate in the posterior flagellar extremity. Bar lengths: A-C and G = 0.4 μm; D-F and I-K = 0.2 μm; H and L-O = 0.1 μm; O = 0.07 μm.

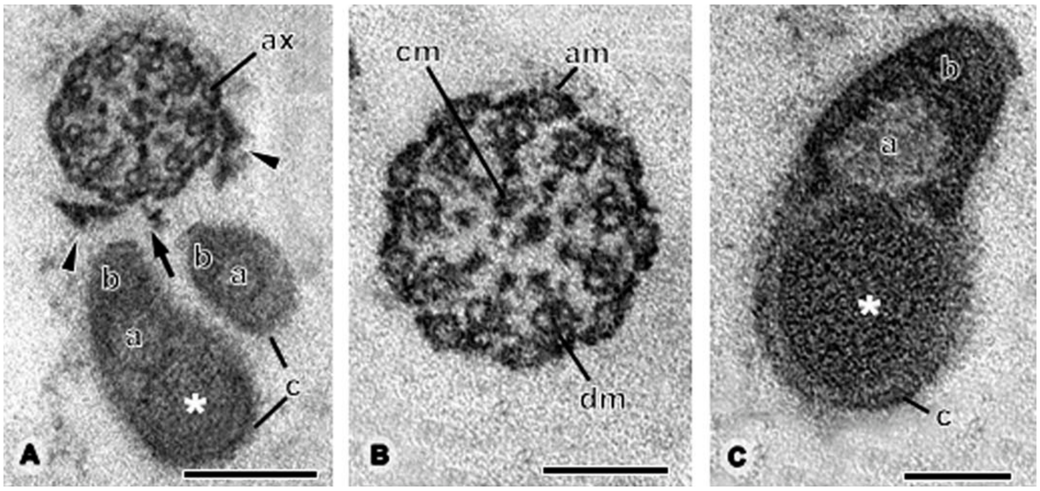

Fig. 3. **A–C**. Transmission electron micrographs of spermatozoa in the seminal vesicle of *M. segmentaria*. Cross section of the flagellum showing the axoneme (ax), accessory bodies (arrowheads) and a central material between the flagellar structures (arrow). Both derivatives have a less dense central region (a), an electron dense region adjacent to the axoneme (b) and a cristae region opposite the axoneme (c). The asterisk indicates a unpublished data paracrystalline region present only on the large derivative. **B**,**C**: Detail of the axoneme and the large mitochondrial derivative. In (B), axoneme with formed by nine accessories microtubule (am), nine doublets (dm) and one central pair (cm); in (C), the large mitochondrial derivative shows the less electron dense (a), more electron dense (b) and cristae (c) regions and the paracrystalline material (asterisk). Bar lengths: A = 0.2 μm; B-C = 0.1 μm.

first, followed by nine doublets and, finally, the accessory microtubules (Figs. 2K–2P).

DISCUSSION

Spermatozoa of *T. analis* and *M. segmentaria* measure 500 μm and 300 μm, respectively, and are within the interval encountered in other bees, which vary from 80 μm in *Scaptotrigona xanthotricha* (Araújo et al., 2005a) to 1500 μm in *Euglossa mandibularis* (Zama et al., 2005a). This large interval of lengths demonstrates that the total length of spermatozoa cannot be used as a valid trait in phylogenic studies because it presents many homoplasies, but is a good taxonomic indicator because it possesses distinct measurements in closely related species (Cruz-Landim, 2008). When observing the length ratio between the nucleus and the flagellum of *T. analis* (0.09) and *M. segmentaria* (0.1), high similarity was observed between species of the tribes Eucerini and Emphorini, respectively. In other phylogenetically related tribes Apinae, nucleus/flagellum length ratios of 0.6 in *Exomalopsis auropilosa* (Exomalopsini) and 0.7 in *Paratetrapedia (Lophopedia)* sp. (Tapinotaspidini) were also very similar (Báo et al., 2004). Therefore, it is necessary to analyze the nucleus/flagellum length ratio in a number of species to confirm whether this ratio remains similar in closely related groups.

The presence of spermatozoa remaining in bundles in the seminal vesicle has been observed in all symphyta species studies (Lino-Neto et al., 2008a; Newman and Quicke, 1999; Quicke et al., 1992) and bundles or its fragments have also been observed in the seminal vesicle of Aculeata (Moreira et al., 2004, 2008; Zama et al., 2004). However, in bees and Aculeata in general, when individuals become sexually mature, bundles begin to break down and are rarely observed in the seminal vesicle. Rather, the presence of individual spermatozoa is more common, which can then be transferred to the female. This characteristic represents a synapomorphy for bees and the Aculeata. This is because in all observed symphyta, the spermatozoa are observed in bundles in the seminal vesicle (Lino-Neto et al., 2008a; Newman and Quicke, 1999; Quicke et al., 1992). Lino-Neto et al. (2008a) suggested that conservation of these bundles in the seminal vesicle of the symphyta, may possibly be related to enzyme content and/or pH of fluids present in the lumen.

In the testes, organization of the germinative cells in cysts is a characteristic common to insects. The number of spermatozoa in the bundle surely represents the final number of cells that develop in synchrony, within the cysts, from a single spermatogonial cell (Lino-Neto et al., 2008b). In bees, males are haploid and during spermatogenesis, at least half of the spermatids are nonviable cells (Conte et al., 2005; Cruz-Landim and Beig, 1980a,b; Cruz-Landim, 2001; Lino-Neto et al., 2008b). However, in *T. analis* and *M. segmentaria*, an average of 50 spermatozoa in each bundle indicates the occurrence of six mitotic cell divisions, as observed for the majority of bees. An exception is the tribe Meliponini, which possesses 128 spermatozoa per bundle, indicating seven mitotic cycles which can be considered a derived trait within this family.

Spermatozoa from *T. analis* and *M. segmentaria* present various similarities with those previously described for other Apidae species. In bees, the acrosome measures 1–2 μm and is formed by the acrosomal vesicle and the perforatorium (Araújo et al., 2005a; Báo et al., 2004; Fiorillo et al., 2005; Zama et al., 2001, 2004, 2005a), with the exception of *Apis mellifera*, in which the acrosome is exceptionally long, and measures 5.6 μm (Cruz-Hofling et al., 1970; Hoage and Kessel, 1968; Lensky et al., 1979; Woyke, 1984). In cross section, the acrosome generally varies from a circular shape in the anterior region, to an ellipsoidal shape in the posterior region, except in Meliponini, in which the posterior region is triangular (Araújo et al., 2005a; Zama et al., 2001, 2004). The acrosomal vesicle, which is formed by lamella in *T. analis* and *M. segmentaria,* has not been found in other bee species. The perforatorium is compact, as in other Apini (Báo et al., 2004), Euglossini (Zama et al., 2005a), and Meliponini (Araújo et al., 2005; Zama et al., 2001, 2004). In Halictinae (Fiorillo et al., 2005), the perforatorium is paracrystalline. The base of the perforatorium inserted in an anterior external cavity of the nucleus is a characteristic observed in practically all Hymenoptera, and therefore, it can be considered a synapomorphic trait of this order.

In spermatozoa from the majority of bee species, nuclear chromatin is very electron dense and compact. However, in *T. analis* and *M. segmentaria* it presents various electron lucid lacunae, as observed in Exomalopsini and Tapinotaspidini (Báo et al., 2004), and in Halictidae, numerous paracrystalline inclusions are observed (Fiorillo et al., 2005). In *Melipona marginata* and *M. rufiventris* (Meliponini), the chromatin is compacted in cloys, giving the nucleus a flaccid chromatin appearance (Zama et al., 2004). An asymmetric projection on the posterior portion of the nucleus is a synapomorphic trait shared among bees. In this transition region, the nucleus is connected to the anterior extremity of the large mitochondrial derivative by a series of electron-dense lamella. In Apidae, the centriolar adjunct initiates at the nuclear base, extends parallel to the axoneme and the large mitochondrial derivative, and terminates at the tip of the small mitochondrial derivative (asymmetric pattern). This is a synapomorphic trait for this family. In general, the centriolar adjunct is electron-dense and compact, its length varying from 2–7 μm in Meliponini (Araújo et al., 2005a; Zama et al., 2001, 2004) to 30 μm in *Apis mellifera* (Lino-Neto et al., 2000). Among the Aculeata, a symmetric centriolar adjunct, when preceding both mitochondrial derivatives, was encountered in Crabronidae wasps (Araújo et al., 2009; Zama et al., 2005b), which is considered a sister group to bees, as well as in ants (Lino-Neto and Dolder, 2002; Moya et al., 2007).

Asymmetry of length and diameter in the mitochondrial derivatives are synapomorphic traits for Apidae. In other Aculeata, such as *Microstigmus* (Zama et al., 2007) and in ants (Lino-Neto and Dolder, 2002; Moya et al., 2007), the mitochondrial derivatives are symmetric. However, in bees the asymmetric diameter of the mitochondrial derivatives is very evident since the large derivative is up to three times greater than the small derivative, as observed in Euglossini (Zama et al., 2005a). In *T. analis* and *M. segmentaria* the derivatives presents a pear-shaped format, and this is also evident in Euglossini (Zama et al., 2005a) and Meliponini (Araújo et al., 2005a; Zama et al., 2001, 2004). In Halictidae (Fiorillo et al., 2005), the derivatives are oval-shaped. Another synapomorphic trait of bees is the presence of paracrystalline material in the large mitochondrial derivative, in the region opposite the axoneme.

In insects in general, the axoneme presents a 9 + 9 + 2 microtubule arrangement and begins with the centriole in the anterior region of the flagellum. At the end of the flagellum, the axoneme is gradually disorganized in most Aculeata: the central pair first terminates, followed by the nine doublets and lastly, the accessory bodies (Araújo et al., 2005a; Báo et al., 2004; Fiorillo et al., 2005; Lino-Neto et al., 2000; Mancini et al., 2006; Zama et al., 2001, 2004, 2005a,b,c, 2007). In ants, they terminate approximately at the same point (Lino-Neto and Dolder, 2002; Wheeler et al., 1990), and in parasitic wasps (Chalcidoidea), the accessories microtubule terminate first (Lino-Neto et al., 1999).

Accessory bodies have a triangular shape and are inserted between the mitochondrial derivatives and the axoneme, but not between the axoneme and the centriolar adjunct, as in Aculeata in general (Araújo et al., 2005a; Báo et al., 2004; Fiorillo et al., 2005; Lino-Neto et al., 2000; Mancini et al., 2006, 2008; Moya et al., 2007; Zama et al., 2001, 2004, 2005a,b,c, 2007).

The two bee species analyzed in this study shared various spermatozoa morphological traits with other previously described bee species. These similarities allow for establishment of a general pattern for the family based on the synapomorphic characteristics: (1) spermatozoa bundle disassembly in the seminal vesicle; (2) perforatorium insertion in a small cavity at the anterior tip of the nucleus; (3) a lateral projection in the posterior region of the nucleus; (4) asymmetric centriolar adjunct; (5) asymmetry of the mitochondrial derivatives and the paracrystalline region in the large derivative; (6) termination sequence of the microtubules and (7) triangular shape of the accessory bodies. The synapomorphies not only establish a general pattern for spermatozoa in Apidae but also reinforce the proposal of Brothers (1999) and Melo (1999), which states that all bees are grouped in the single family Apidae.

ACKNOWLEDGMENTS

The authors would like to acknowledge the *Núcleo de Microscopia e Microanálise* of the Federal University of Viçosa (UFV) and the *Laboratório de Microscopia Eletrônica* of the University of Brasília (UnB).

REFERENCES

Araújo VA, Zama U, Dolder H, Lino-Neto J. 2005a. Morphology and ultrastructure of the spermatozoa of *Scaptotrigona xanthotricha* Moure (Hymenoptera. Apidae, Meliponini). Braz J Morphol Sci 22:137–141.

Araújo VA, Zama U, Neves CA, Dolder H, Lino-Neto J. 2005b. Ultrastructural, histological and histochemical characteristics of the epithelial wall of the seminal vesicle of mature *Scaptotrigona xanthotricha* Moure males (Hymenoptera. Apidae, Meliponini). Braz J Morphol Sci 22:129–137.

Araújo VA, Moreira J, Lino-Neto J. 2009. Structure and ultrastructure of the spermatozoa of *Trypoxylon (Trypargilum) albitarse Fabricius* 1804 (Hymenoptera: Apoidea: Crabronidae). Micron 40:719–723.

Baccetti B. 1970. The spermatozoon of Arthropoda. In: Baccetti B, editor. The sperm cell as an index of arthropod phylogenesis. Comparative spermatology. New York: Academic Press. pp.169–182.

Báo SN, Gonçalves-Simões D, Lino-Neto J. 2004. Sperm ultrastructure of the bees *Exomalopsis (Exomalopsis) auropilosa* Spinola 1853 and *Paratetrapedia (Lophopedia)* sp. Michener & Moure 1957 (Hymenoptera, Apidae, Apinae). J Submiscrosc Cytol Pathol 36:23–28.

Brothers DJ. 1999. Phylogeny and evolution of wasps, ants and bee (Hymenoptera. Chrysidoidea, Vespoidea and Apoidea). Zool Scr 28:233–249.

Conte MJ, Lino-Neto J, Dolder H. 2005. Spermatogenesis of Melipona quadrifasciata anthidioides (Hymenoptera: Apidae): Fate of the atypical spermatids. Caryologia 58:183–188.

Cruz-Ladim C, Beig D. 1980a. Meiose nos Hymenoptera. Ciência e Cultura 33:937–966.

Cruz-Ladim C, Beig D. 1980b. An electron microscopic study of spermatogenesis in the drone of *Scaptotrigona postica* (Hymenoptera: Apidae). Inter J Inver Rep 2:271–283.

Cruz-Landim C. 2001. Organization of the cysts in bee (Hymenoptera. Apidae) testis: Number of spermatozoa per cyst. Iheringia 91:183–189.

Cruz-Landim C. 2008. Abelhas: Morfologia e função de sistemas. São Paulo: Editora Unesp. pp. 407.

Cruz-Hofling MA, Cruz-Landim C, Kitajima EW. 1970. The fine structure of spermatozoa from the honey bee. An Acad Bras Ciên 42:69–78.

Dallai R. 1974. Spermatozoa and phylogenesis. A few data on Insecta Apterygota. Pedobiologia 14:148–156.

Dallai R, Afzelius BA. 1993. Development of the accessory tubules of insect sperm flagella. J Submiscrosc Cytol Pathol 25:499–504.

Fiorillo BS, Coelho AAM, Lino-Neto J, Báo SN. 2005. Structure and ultrastructure of the spermatozoa of Halictidae (Hymenoptera. Apoidea). J Submicrosc Cytol Pathol 37:75–81.

Gracielle IMS, Fiorillo BS, Lino-Neto J, Báo xSN. 2009. Morphology of the male reproductive system and spermiogenesis in *Hypanthidium foveolatum* (Alfken, 1930) Hymenoptera: Apidae: Megachilinae. Micron 40:419–425.

Hoage TR, Kessel RG. 1968. An electron microscope study of the process of differentiation during spermatogenesis in the drone honey bee (*Apis mellifera L.*) with special reference to centriole replication and elimination. J Ultrastruct Res 24:6–32.

Jamieson BGM. 1987. The ultrastructure and phylogeny of insect spermatozoa. Cambridge: Cambridge University Press.

Jamieson BGM, Dallai R, Afzelius BA. 1999. Insects: Their spermatozoa and phylogeny. Enfield: Scientific publishers.

Lensky Y, Ben-David E, Schindler H. 1979. Ultrastructure of the spermatozoa of the mature drone honey bee. J Apic Res 18:264–271.

Lino-Neto J, Báo SN, Dolder H. 1999. Structure and ultrastructure of the spermatozoa of *Bephratelloides pomorum (Fabricius)* (Hymenoptera: Eurytomidae). Int J Insect Morphol Embryol 28:253–259.

Lino-Neto J, Báo SN, Dolder H. 2000. Sperm ultrastructure of the honey bee (*Apis mellifera*) (L) (Hymenoptera. Apidae) with emphasis on the nucleus-flagellum transition region. Tissue Cell 32:322–327.

Lino-Neto J, Dolder H. 2002. Sperm structure and ultrastructure of the fire ant *Solenopsis invicta Bauren (Hymenoptera. Formicidae)*. Tissue Cell 34:124–128.

Lino-Neto J, Dolder H, Mancini K, Mercati D, Dallai R. 2008a. The short spermatodesm of *Arge pagana* (Hymenoptera: symphyta). Tissue Cell 40:185–193.

Lino-Neto J, Araújo VA, Dolder H. 2008b. Inviability of the spermatids with little cytoplasm in bees (Hymenoptera. Apidae). Sociobiology 51:163–172.

Mancini K, Lino-Neto J, Dolder H. 2006. Sperm ultrastructure of *Agelaia vicina (Hymenoptera: Vespidae)*. Insect Soc 53:333–338.

Mancini K, Lino-Neto J, Dolder H, Dallai R. 2008. Sperm ultrastructure of the European hornet *Vespa crabro (Linnaeus, 1758) (Hymenoptera: Vespidae)*. Arthropod Struct Dev 38:54–59.

Melo GAR. 1999. Phylogenetic relationships and classification of the major lineages of Apoidea (Hymenoptera) with emphasis on the crabronid wasps. Mus Nat His Univ Kansas 14:1–55.

Moreira J, Zama U, Lino-Neto J. 2004. Release, behavior and phylogenetic significance of spermatozoa in bundles in the seminal vesicle during sexual maturation in Aculeata (Hymenoptera). Braz J Morphol Sci 21:185–189.

Moreira PA, Araújo VA, Zama U, Lino-Neto J. 2008. Morphology of male reproductive system in three species of *Trypoxylon* (*Trypargilum*) Richards (Hymenoptera: Crabronidae). Neotrop Entomol 37:429–435.

Moya J, Mancini K, Lino-Neto J, Delabie J, Dolder H. 2007. Sperm ultrastructure of five species of the Neotropical ant genus *Pseudomyrmex (Hymenoptera: Formicidae)*. Acta Zool 88:181–187.

Newman TM, Quicke DLJ. 1999. Ultrastructure of imaginal spermatozoa of sawflies (Hymenoptera: Symphyta). J Hym Res 8:35–47.

Peng CYS, Yin CM, Yin LRS. 1992. Effect of rapid freezing and thawing on cellular integrity of honey bee sperm. Physiol Entomol 17:269–276.

Peng CYS, Yin CM, Yin LRS. 1993. Ultrastructure of honey bee. Apis mellifera sperm with special emphasis on the acrosomal complex following high-pressure freezing fixation. Physiol Entomol 18:93–101.

Phillips DM. 1970. Insect flagellar tubule patterns theme and variations. In: Baccetti B, editor. Comparative spermatology. New York: Academic Press. pp. 263–278.

Quicke DLJ, Ingram SN, Baillie HS, Gaitens PV. 1992. Sperm structure and ultrastructure in the Hymenoptera (Insecta). Zool Scr 21:381–402.

Rothschild L. 1955. The spermatozoa of the honey bee. Trans Roy Ent Soc Lond 107:289–294.

Wheeler DE, Crichton ED, Krutzsch PH. 1990. Comparative ultrastructure of ant spermatozoa (Formicidae: Hymenoptera). J Morphol 206:343–350.

Woyke J. 1984. Ultrastructure of single and multiple diploid honey bee spermatozoa. J Hym Res 23:123–135.

Zama U, Lino-Neto J, Dolder H. 2001. Ultrastructure of spermatozoa in *Plebeia (Plebeia) droryana Friese* (Hymenoptera: Apidae: Meliponina). J. Hym. Res. 10:261–270.

Zama U, Lino-Neto J, Dolder H. 2004. Structure and ultrastructure of spermatozoa in Meliponini (Stingless bees) (Hymenoptera: Apidae). Tissue Cell 36:29–41.

Zama U, Lino-Neto J, Melo SM, Campos LAO, Dolder H. 2005a. Ultrastructural characterization of spermatozoa in Euglossini bees (Hymenoptera: Apidae: Apinae). Insect Soc 52:122–131.

Zama U, Bottura G, Lino-Neto J, Dolder H, Báo SN. 2005b. The nucleus e flagellum transition in *Trypoxylon* (*Trypargilum*) subgenus, with emphasis on a singular centriolar adjunct (Hymenoptera: Apoidea: Crabronidae). Braz J Morphol Sci 22(Suppl.): 56–57.

Zama U, Brito P, Lino-Neto J, Campos LAO, Dolder H, Báo SN. 2005c. The sperm morphology of mud dauber *Sceliphron fistularium* Dahlbom (Hymenoptera: Apoidea: Sphecidae), as an indicative of bees relation. J Submicrosc Cytol Pathol 37:91–99.

Zama U, Moreira JCS, Báo SN, Campos LAO, Dolder H, Lino-Neto J. 2007. Morphology of testicular and post-testicular spermatozoa in *Microstigmus arlei* Richards, 1972 and *M. nigrophthalmus Melo,* 1992 (Hymenoptera: Apoidea: Pemphredoninae) with phylogenetic consideration. Arthropod Struct Dev 36:304–316.